THROMBOSIS AND HEMOSTASIS

Desmolaris, a novel factor XIa anticoagulant from the salivary gland of the vampire bat (*Desmodus rotundus*) inhibits inflammation and thrombosis in vivo

Dongying Ma,[1] Daniella M. Mizurini,[2] Teresa C. F. Assumpção,[1] Yuan Li,[1] Yanwei Qi,[3] Michail Kotsyfakis,[4] José M. C. Ribeiro,[1] Robson Q. Monteiro,[2] and Ivo M. B. Francischetti[1]

[1]Vector Biology Section, Laboratory of Malaria and Vector Research, National Institute of Allergy and Infectious Diseases, National Institutes of Health, Bethesda, MD; [2]Instituto de Bioquímica Médica, Universidade Federal do Rio de Janeiro, Rio de Janeiro, Brazil; [3]Malaria Functional Genomics Section, Laboratory of Malaria and Vector Research, National Institute of Allergy and Infectious Diseases, National Institutes of Health, Bethesda, MD; and [4]Institute of Parasitology, Biology Centre of the Academy of Sciences of Czech Republic, České Budějovice, Czech Republic

Key Points

- Desmolaris, a major anticoagulant from vampire bat saliva, has been identified as a novel FXIa inhibitor.
- Desmolaris inhibits arterial thrombosis at concentrations that does not impair hemostasis.

The identity of vampire bat saliva anticoagulant remained elusive for almost a century. Sequencing the salivary gland genes from the vampire bat *Desmodus rotundus* identified Desmolaris as a novel 21.5-kDa naturally deleted (Kunitz 1-domainless) form of tissue factor pathway inhibitor. Recombinant Desmolaris was expressed in HEK293 cells and characterized as a slow, tight, and noncompetitive inhibitor of factor (F) XIa by a mechanism modulated by heparin. Desmolaris also inhibits FXa with lower affinity, independently of protein S. In addition, Desmolaris binds kallikrein and reduces bradykinin generation in plasma activated with kaolin. Truncated and mutated forms of Desmolaris determined that Arg32 in the Kunitz-1 domain is critical for protease inhibition. Moreover, Kunitz-2 and the carboxyl-terminus domains mediate interaction of Desmolaris with heparin and are required for optimal inhibition of FXIa and FXa. Notably, Desmolaris (100 μg/kg) inhibited $FeCl_3$-induced carotid artery thrombus without impairing hemostasis. These results imply that FXIa is the primary in vivo target for Desmolaris at antithrombotic concentrations. Desmolaris also reduces the polyphosphate-induced increase in vascular permeability and collagen- and epinephrine-mediated thromboembolism in mice. Desmolaris emerges as a novel anticoagulant targeting FXIa under conditions in which the coagulation activation, particularly the contact pathway, plays a major pathological role. (*Blood*. 2013;122(25):4094-4106)

Introduction

Blood coagulation cascade is a physiological mechanism that is triggered to avoid blood loss.[1,2] Coagulation is initiated by 2 pathways that work in concert through a number of reactions of limited proteolysis. The extrinsic pathway is initiated by factor (F) VIIa/tissue factor with formation of FXa (extrinsic Xnase) that assembles in the prothrombinase complex, resulting in activation of prothrombin to thrombin.[3] Alternatively, the contact pathway is initiated by negatively charged molecules that activate FXII, and FXIIa cleaves and activates prekallikrein (PK).[4,5] FXIIa also activates FXI, and FXIa activates FIXa. The FIXa assembles in the intrinsic Xnase complex and activates FX to FXa, leading to thrombin generation.[3-5] In addition, FXI is activated by thrombin in the surface of platelets[3,6] or negatively charged molecules[7,8] and has emerged as an important pathway for consolidation of the clotting cascade.[1,2] FXIa also plays a particularly important role in thrombus formation in vivo.[9-11]

The coagulation cascade is regulated by several plasma inhibitors, including tissue factor pathway inhibitor (TFPI), activated protein C, antithrombin, heparin cofactor II, protease nexin I and II, C1 inhibitor, α-1-protease inhibitor, and α-2-antiplasmin.[1,2,12,13] Several other coagulation inhibitors have been characterized from hematophagous animals.[14-16] Among these, vampire bats (eg, *Desmodus rotundus*) are the sole mammals that feed exclusively on blood. Accordingly, bat saliva has historically been associated with hematophagous behavior.[17] For example, the presence of anticoagulant and fibrinolytic activity in vampire bat saliva was first suggested by Bier in 1932.[18] Inhibition of platelet aggregation and vasodilation properties was later described in the salivary secretion.[19] In regard to anticoagulant activity, a protein purified from saliva (named Draculin) and identified as lactotransferrin (based on the N terminus) was proposed as the anticoagulant of the gland.[20] Because lactotransferrin is a well-known antimicrobial, and because it has not been obtained in recombinant form, the true identity of the bat anticoagulant remained elusive for almost a century. Actually, the only molecule that has been molecularly and functionally characterized so far in bat saliva is the plasminogen activator desmoteplase, which has been tested in clinical trials as a thrombolytic for the treatment of ischemic stroke.[21]

More recently, the first comprehensive transcriptome analysis and proteome studies of *D. rotundus* submaxillary glands were reported.[22]

Submitted August 5, 2013; accepted October 21, 2013. Prepublished online as *Blood* First Edition paper, October 24, 2013; DOI 10.1182/blood-2013-08-517474.

The online version of this article contains a data supplement.

The publication costs of this article were defrayed in part by page charge payment. Therefore, and solely to indicate this fact, this article is hereby marked "advertisement" in accordance with 18 USC section 1734.

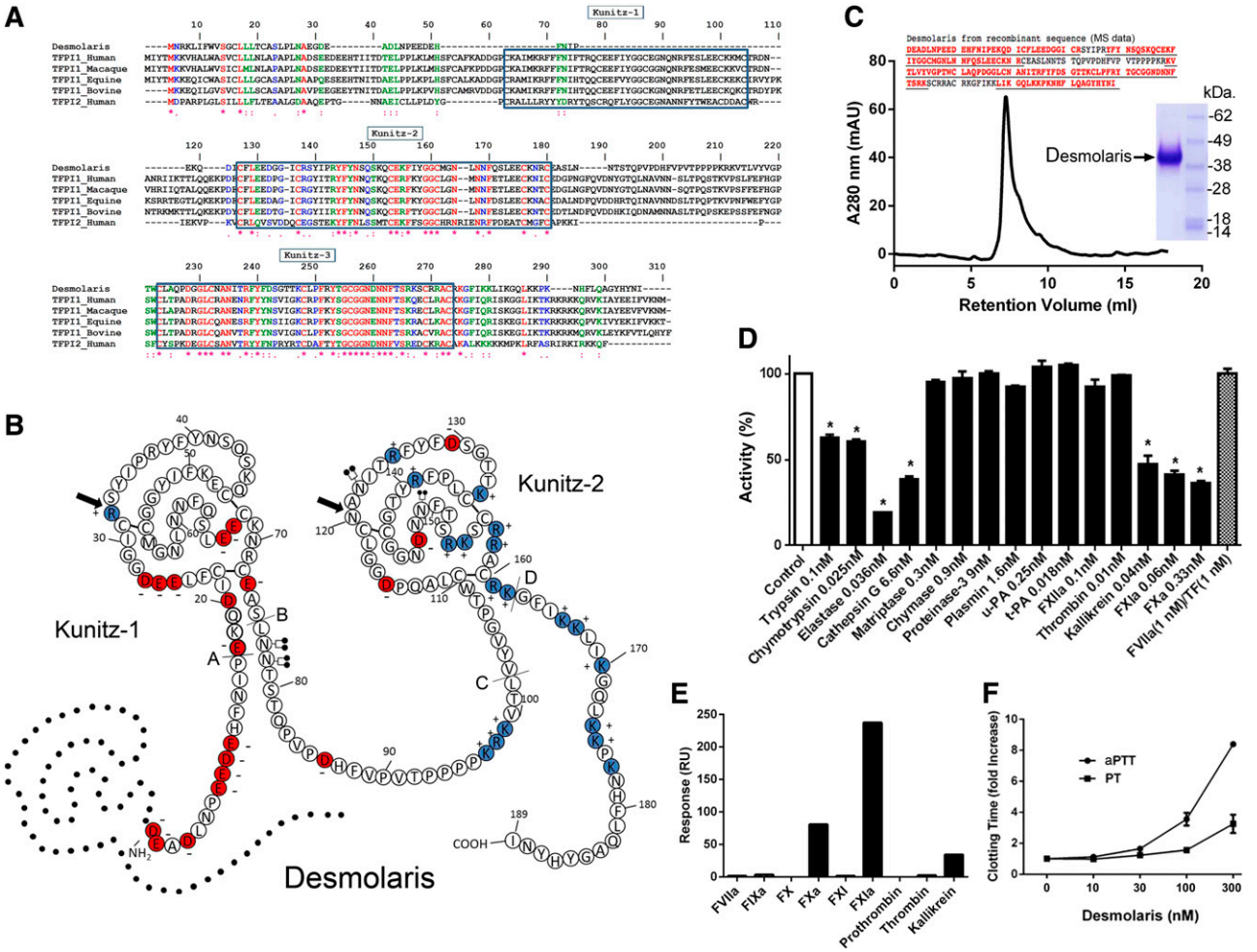

Figure 1. Desmolaris is a major anticoagulant from vampire bat saliva. (A) Clustal alignment. Desmolaris (gi527498655) and TFPI-1 from *Homo sapiens* (gi5454114), *Macaca mullatta* (gi297264502), *Equis cabalus* (gi338715615), *Bos taurus* (gi346644729), and TFPI-2 from *Homo sapiens* (gi5730091) were aligned. (B) Predicted secondary structure of Desmolaris based on human TFPI.[12] Amino acids are identified by a single letter code. Basic (positively charged) residues are colored in blue and acidic (negatively charged) residues in red. Arrows indicate P_1 sites. N glycosylation sites were found for Asn77, Asn 78, Asn 122, and Asn 149. Putative phosphorylation sites were identified at Ser 42, Thr 133, Thr 141, Thr 151, Ser 152, and Ser 155. The Kunitz domains are labeled. Dotted lines correspond to Kunitz-1 of TFPI. The putative sites of introns in the Desmolaris gene (based in human TFPI)[12] are labeled with lines and the capital letters A, B, C, and D. (C) Recombinant expression. Desmolaris was expressed in HEK293 cells and purified with an Ni^{2+} column followed by reverse-phase chromatography. (Inset) Samples were loaded in a NuPAGE gel under reducing conditions. Gels were stained with Coomassie Blue. Molecular mass markers are shown (right). The arrow indicates Desmolaris. The Desmolaris sequences depicted in red and underlined are the peptides identified by mass spectrometry, with more than 70% coverage. (D) Screening for enzyme inhibition by Desmolaris. Enzymes at indicated concentrations were incubated with Desmolaris (250 nM), and catalytic activity was estimated by fluorogenic substrate hydrolysis. FVIIa/TF complex activity was determined with chromogenic substrate (S2366). Results are the mean ± standard error of triplicates. (E) SPR experiments. Desmolaris was immobilized in a CM5 chip, and several coagulation enzymes and zymogens (all at 64 nM) were injected as analytes. Association phase of 60 seconds was followed by a 60-second dissociation. Resonance values are based on binding at stability. A typical result is shown. (F) PT and aPTT. Desmolaris was added to plasma at the indicated concentrations, followed by addition of a PT or aPTT reagent as described in the "Methods" section. Clotting was estimated using a coagulometer. Control human plasma: PT, 14.6 ± 0.20 seconds; aPTT, 35.9 ± 0.15 seconds (each data point is the average of duplicate or triplicate determinations).

This database of more than 8000 proteins revealed that the bat salivary gland expresses a much more complex mixture of molecules than previously thought. Several putative inhibitors acting on platelets, neutrophils, and the clotting cascade—in addition to vasodilators—have been identified.[22] Among these molecules, a 2-Kunitz-domain type inhibitor named Desmolaris exhibited similarity to TFPI, the inhibitor of the extrinsic pathway of the coagulation cascade.[12] Our results demonstrate that Desmolaris is a naturally deleted Kunitz-1-domainless form of TFPI that tightly binds FXIa.

Methods

All experiments were performed as described in detail in the supplemental Methods, available on the *Blood* Web site. All in vivo experiments described follow the rules for animal experimentation and care. Protocols Laboratory of Malaria and Vector Research-3 were approved by the National Institute of Allergy and Infectious Diseases Internal Review Board of the National Institutes of Health, National Institute of Allergy and Infectious Diseases; and protocol IBqM081- 05/16 was approved by the Institute of Medical Biochemistry at Federal University of Rio de Janeiro.

Results

Desmolaris is a major anticoagulant of vampire bat saliva

Desmolaris complementary DNA (gi 527498656) was initially sequenced from the salivary gland of the vampire bat *D. rotundus*.[22] Figure 1A shows the sequence of Desmolaris. It is a 21.5-kDa

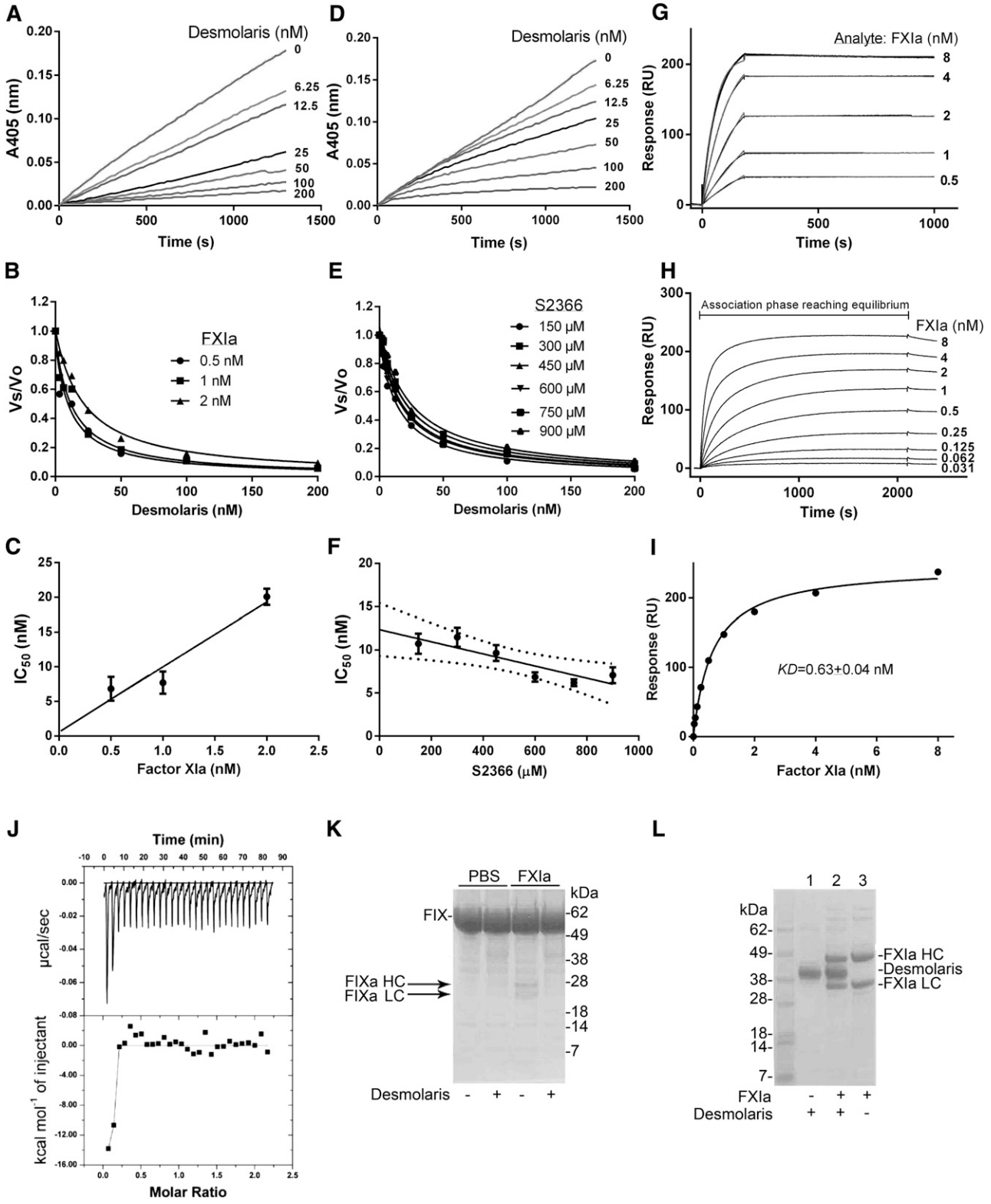

Figure 2. Desmolaris is a slow and tight inhibitor of FXIa. (A) Inhibition of the catalytic activity of FXIa. Reactions started by addition of S2366 (250 μM) to a mixture containing Desmolaris (0-200 nM) incubated for 1 hour with FXIa (0.5 nM). Substrate hydrolysis was followed for 2 hours at 405 nm. (B) Tight inhibition. Experiments were performed as in (A) but at 0.5, 1, and 2 nM FXIa. The rate of substrate hydrolysis between 30 and 60 minutes (*Vmax* mode) was transformed as *Vs*/*Vo* and plotted against Desmolaris concentration. Data points were fitted with the Morrison equation to calculate the IC_{50} at each enzyme concentration. (C) Plot of IC_{50} and FXIa produces a straight line typical of tight inhibitors. (D) Slow-type inhibition. Reactions started with addition of FXIa (0.5 nM) to a mixture containing Desmolaris and S2366 (250 μM). Substrate hydrolysis was followed for 2 hours at 405 nm. (E) IC_{50} determination. FXIa was added to Desmolaris in the presence of S2366 (150, 300, 450, 600, 750, and 900 μM). The ratio *Vs*/*Vo* obtained (*Vmax* mode) between 30 and 60 minutes was plotted against S2366 concentrations. Data were fitted with the Morrison equation to calculate the IC_{50} values at each substrate concentration. Six experiments were performed, and each data point is the average of duplicate determinations. Confidence interval is shown as dotted lines. (F) Determination of the K_i: plot of IC_{50} vs S2366 concentrations was fitted by linear regression and the *y* intercept equals the K_i. (G) SPR experiments. Factor XIa at the indicated concentrations was injected over immobilized Desmolaris for 180 seconds. Dissociation of the Desmolaris-FXIa complex was monitored for 900 seconds.

protein, pI 8.57 containing 2-Kunitz domains, an acidic N terminus, and a basic carboxy-terminus. Clustal alignment with TFPI-1 from human, macaque, equine, bovine, and human TFPI-2 shows that Desmolaris does not contain a sequence corresponding to the Kunitz-1 domain of TFPI.[23] Alignment also reveals that the first and second Kunitz of Desmolaris correspond to the second and third domains of TFPI, respectively. In the Kunitz-1 of Desmolaris, the P_1 position is occupied by an Arg, whereas in the Kunitz-2 it is an Asn. In TFPI, all P_1 positions are occupied by Arg.[23] In regard to other residues, Kunitz-1 of Desmolaris and Kunitz-2 of TFPI are highly conserved. In contrast, several residues present in Desmolaris Kunitz-2 (eg, Gln113, Gly116, Asp120, Iso123, Gly131, Thr132, Thr133) have been replaced by other residues in the Kunitz-3 of TFPI (Figure 1A). Figure 1B reveals the predicted secondary structure of Desmolaris, based on the structure determined for TFPI.[12] Desmolaris contains 4 N-linked glycosylation sites at Asn77, Asn78, Asn122, and Asn149. The putative sites of introns in the Desmolaris gene, based on TFPI,[12] are labeled with lines and capital letters A-D.

To determine its function, Desmolaris was expressed in HEK293 cells, purified to homogeneity (Figure 1C), and migrated as a 38-kDa protein (inset). This molecular mass is greater than predicted by the complementary DNA and is compatible with four N-glycosylation sites. Identity of Desmolaris was confirmed by mass spectrometry analysis with coverage above 70% (Figure 1C inset; peptide sequences obtained by mass spectrometry, analysis available in the supplemental Methods). Screening assay shows that Desmolaris inhibits FXa, FXIa, and kallikrein but does not affect thrombin, FXIIa, plasmin, tissue- and urokinase-type plasminogen activators, matriptase, chymase, or proteinase 3 at large molar excess (Figure 1D). Colorimetry assays with chromogenic substrates (S2366) also determined that Desmolaris (1 μM) does not affect FVIIa (1 nM)/TF (1 nM) amidolytic activity. Desmolaris was also found to inhibit other enzymes such as trypsin, α-chymotrypsin, and neutrophil-derived elastase and cathepsin G.

Next, Desmolaris was immobilized in a CM5 chip followed by injection of coagulation factors as analytes. Figure 1E demonstrates that only FXIa, FXa, and kallikrein bind to Desmolaris, whereas the zymogens FIX, FX, FXI, and FXII and the enzymes FVIIa and FIXa do not. Coagulation tests were then performed. Figure 1F shows that Desmolaris dose-dependently prolongs the prothrombin time (PT) and the activated partial thromboplastin time (aPTT). At 300 nM, Desmolaris increases the PT twofold. In contrast, Desmolaris at the same concentration prolongs the aPTT ninefold.

Desmolaris is a slow, tight, and noncompetitive inhibitor of FXIa

The kinetics of the interaction of Desmolaris and FXIa with a small chromogenic substrate S2366 was examined. To determine whether the interaction is tight, Desmolaris (0-200 nM) and FXIa (0.5 nM) were incubated for 1 hour followed by addition of S2366 (250 μM). Figure 2A shows that Desmolaris inhibits S2366 cleavage in a dose-dependent manner. A similar experiment was performed using FXIa at 0.5, 1, and 2 nM. The rate of substrate hydrolysis between 30 and 60 minutes (*Vmax* mode) was transformed as the final velocity, inhibited enzyme (*Vs*) to the initial velocity, uninhibited enzyme (*Vo*), or *Vs/Vo*, and fitted with the Morrison equation for tight inhibitors, which allows calculation of the 50% inhibition/inhibitory concentration (IC_{50}) at each condition (Figure 2B).[24-26] A plot of the IC_{50} and FXIa indicates that inhibition was attained at similar concentrations of the reactants, compatible with tight inhibition (Figure 2C).

To characterize the interaction as slow or fast, the enzyme was added to a reaction mixture containing the inhibitor and S2366. Figure 2D shows progression curves displaying a downward concavity followed by a linear component after 10 minutes, which indicates that after a first encounter, the reaction proceeds to formation of a final, stable complex when it reaches a steady state ($E+I \leftrightarrow EI \leftrightarrow EI^*$). This kinetic pattern is typical of slow-binding inhibitors. To determine the type of inhibition (competitive vs noncompetitive),[23,27,28] *Vs/Vo* values were obtained between 30 and 60 minutes (*Vmax* mode) and fitted with the Morrison equation for 6 substrate concentrations. Figure 2E shows that the curves obtained using this approach were almost superimposable, resulting in similar IC_{50} values. To determine the equilibrium inhibition constant (K_i), the IC_{50} values obtained were plotted against each substrate concentration and a linear regression was used to fit the data points (Figure 2F). The y-axis intercept determines the K_i as 12.35 ± 1.09 nM, which is the K_i in the limiting condition of substrate absence.[23,27,28] The pattern depicted in Figure 2F indicated that Desmolaris as a noncompetitive inhibitor of FXIa with respect to S2366.

Surface plasmon resonance (SPR) experiments were then performed. Figure 2G shows that FXIa readily associates with immobilized Desmolaris followed by slow dissociation of the complex. Interaction is noncovalent because complete dissociation was observed after injection of an acidic solution needed to regenerate the sensor chip. The equilibrium dissociation constant (*KD*) was initially calculated kinetically using the ratio of the dissociation rate constant (*koff*) to the association rate constant (*kon*), or *koff/kon*. Sensorgram analysis for the interactions of FXIa with immobilized Desmolaris resulted in *kon* $1.866 \pm 0.002 \times 10^6\ M^{-1}/s^{-1}$ and *koff* $5.567 \pm 0.094 \times 10^{-5}/s^{-1}$, with *KD* 30 pM. However, this value is not accurate because of the slow *koff* that approached the limits that the instrument can reliably measure. Increasing the dissociation time to 7 hours did not improve the values calculated kinetically. Likewise, when Desmolaris was used as an analyte for immobilized FXIa, the affinity was also found to be tight with an unreliable *koff* (not shown).

To accurately estimate the *KD*, the association phase of FXIa interaction with immobilized Desmolaris was allowed to proceed for 30 minutes, which was the time needed for complex formation to reach equilibrium binding (steady state) (Figure 2H). This approach is particularly useful using SPR because it allows the concentrations

Figure 2 (continued) Representative sensorgrams are shown in black lines; global fitting using the Langmuir equation is depicted in red lines. (H) Equilibrium binding. FXIa was injected for 30 minutes into immobilized Desmolaris, allowing complex formation to reach equilibrium. Representative experiment is illustrated. (I) Steady-state affinity. The resonance values obtained at binding stability (30 minutes of association phase) in panel H were plotted against FXIa concentration, and *KD* 0.63 ± 0.04 nM was determined. (J) Solution binding of Desmolaris to FXIa by ITC. (Upper panel) Baseline-adjusted heats per injection of FXIa (10 μM) into Desmolaris (1.0 μM). (Lower panel) Molar enthalpies per injection for FXIa interaction with Desmolaris. Filled squares, measured enthalpies; solid line, fit of experimental data to a single site-binding model. Typical experiment is depicted. (K) Desmolaris inhibits FXIa-mediated FIX activation. Controls (lanes 1 and 2): Recombinant FIX (BeneFIX, 1.2 μM) in the presence of phosphate-buffered saline (PBS) (lane 1) or 300 nM Desmolaris (lane 2). Lanes 3 and 4: FXIa (3 nM) was added to FIX in the presence of PBS (lane 3) or Desmolaris (lane 4) and mixture was incubated for 37°C for 60 minutes. Reactions were stopped with reducing Laemmli buffer, and proteins were separated by 4% to 12% SDS-PAGE. The bands correspond to uncleaved FIX, the heavy chain of FIXa (FIXa HC), and the light chain of FIXa (FIXa LC). Typical gel is shown. (L) Cleavage of Desmolaris. Desmolaris (7.5 μM) was incubated with FXIa (1.7 μM) for 8 hours. The mixture was loaded in a NuPAGE gel under reducing conditions. The bands corresponding to FXIa HC, FXIa LC, or Desmolaris are indicated. Lane 1, Desmolaris; lane 2, FXIa plus Desmolaris; lane 3, FXIa. No cleavage is observed.

of the ligand (eg, FXIa) to remain constant during injection. Therefore, the resonance values at equilibrium (30 minutes) for each analyte concentration are an excellent estimate of complex formation. Accordingly, it reaches a theoretic maximum as the analyte concentration approaches saturation; the half-maximum response is used experimentally to estimate the affinity. Using this approach, *KD* 0.63 nM + 0.04 nM was calculated for the FXIa/Desmolaris complex (Figure 2I).

Isothermal titration calorimetry (ITC) was performed to study the interaction in solution. Binding was exothermic, with a favorable enthalpy (ΔS) of −13.81 Kcal/mol and favorable entropy (TΔS = 1.475 Kcal/mol) (Figure 2J). Fitting of the observed enthalpies revealed a tight *KD* for Desmolaris binding to FXIa with a stoichiometry of ~2:1. However, the tight nature of the interaction precludes a reliable estimation of the *KD* because calculations are limited by the parameter c = Ka [P], where Ka is the association equilibrium constant and [P] is the protein concentration in the calorimeter cell.[27]

FXIa activates FIX to FIXa, and this reaction is accompanied by generation of FIXa's heavy (HC) and light chains (LC).[28] Figure 2K shows that incubation of FXIa with Desmolaris, followed by addition of FIX, results in inhibition of the generation of the bands corresponding to FIXa HC and FIXa LC. To evaluate whether Desmolaris is cleaved by FXIa, the inhibitor was incubated with the enzyme, followed by detection of FXIa (HC and LC). Figure 2L shows that no cleavage of the inhibitor took place.

Desmolaris is a slow, tight, and noncompetitive inhibitor of FXa

Figure 3A shows that Desmolaris preincubated with FXa inhibits the amidolytic activity (tested with S2222) of the enzyme dose-dependently. Figure 3B shows that the IC_{50} increases with FXa concentration. Plot of the IC_{50} and FXa concentrations results in a straight line that is compatible with a tight inhibition (Figure 3C). Figure 3D shows that Desmolaris is a slow-type inhibitor of FXa. Figure 3E-F reveals a noncompetitive type of inhibition of FXa by Desmolaris (with respect to S2222), with a K_i of 15.06 ± 2.5 nM.

SPR experiments are shown in Figure 3G. Best fit was attained using a 1:1 Langmuir equation, with a calculated *kon* 1.831 ± 0.4 × 10^5 M^{-1}/s^{-1} and *koff* 2.95 ± 0.2 × $10^{-3}/s^{-1}$, and *KD* 17.79 + 3.57 nM. Desmolaris also binds to mice FXa (*KD* 47.7 nM; *kon* 1.525 ± 0.9 × 10^5 M^{-1}/s^{-1} and *koff* 7.27 ± 0.2 × $10^{-3}/s^{-1}$). Next, ITCs were performed. Fitting of the observed enthalpies to a single-site–binding model revealed *KD* 16 ± 0.62 nM with a stoichiometry of binding (n = 0.70 ± 0.006), compatible with 1:1 enzyme/inhibitor complex formation (Figure 3H). Binding was endothermic, with an unfavorable enthalpy (ΔH) of 39.52 kcal/mol and favorable entropy (TΔS = 50.3 kcal/mol).

FXa assembles in the prothrombinase complex and promotes prothrombin conversion to thrombin. When the prothrombinase reaction was initiated by addition of prothrombin to a mixture containing preincubated FXa/Desmolaris, a dose-dependent inhibition of thrombin formation was achieved (Figure 3I). In contrast, prothrombinase was not inhibited when reactions were started with prothrombin/Desmolaris (not shown, n = 4). It has been reported that Protein S enhances FXa inhibition by TFPI in the presence of phosphatidylcholine/phosphatidylserine/phosphatidylethanolamine and Ca^{2+}.[29,30] Although Protein S (0-160 nM) increases the inhibition of FXa (0.5 nM) by TFPI, no change was observed with Desmolaris (10 nM) (not shown). Figure 3J shows no change in the migration pattern of Desmolaris or appearance of lower molecular weight bands after incubation with FXa, excluding cleavage.

Desmolaris inhibits kallikrein but not FXIIa

FXIa and kallikrein display sequence homology.[28] We studied whether Desmolaris inhibits the amidolytic activity of kallikrein using S2302. Figure 4A shows partial inhibition of the amidolytic activity, which reaches maximum at approximately 25 nM. Figure 4B shows transformation of the data as *Vs/Vo*. SPR experiments indicate that kallikrein binds to Desmolaris with *KD* 115 ± 5.7 nM (*kon* 6.91 ± 0.36 × 10^4 M^{-1}/s^{-1} and *koff* 7.968 ± 0.018 × $10^{-3}/s^{-1}$; Langmuir equation) (Figure 4C).

FXII (FXIIa) cleaves PK to generate active kallikrein, which in turn reciprocally activates FXII zymogen.[4,5] When reciprocal activation assays were performed in the presence of Desmolaris, dose-dependent inhibition of S2302 hydrolysis was observed, implying that the inhibitor prevents kallikrein activity in vitro (Figure 4D). Control experiments with S2302 excluded inhibition by Desmolaris because of blockade of FXIIa amidolytic activity (Figure 4E). Desmolaris also did not inhibit FXIIa-mediated activation of FXI (Figure 4F). Corn trypsin inhibitor (CTI) blocked the activity of FXIIa in both assays. Next, experiments were optimized in which kaolin—a known activator of FXII—was added to plasma to activate the contact pathway.[4,5] FXIIa activates PK to kallikrein, an enzyme that cleaves HMWK, leading to formation of bradykinin (BK), a potent constrictor of the guinea-pig ileum.[4,5] Figure 4G shows that plasma plus kaolin promote a vigorous contraction, which is similar to 10 ng of BK used as control. When Desmolaris (0.6 μM) was added to the plasma, near complete inhibition was attained. Figure 4H shows a dose-response curve with an IC_{50} ~200 nM.

Heparin is a cofactor for Desmolaris

Figure 5A shows that FXa inhibition by Desmolaris is enhanced by heparin; Figure 5B shows that this effect is dose-dependent. Next, Desmolaris was incubated with FXa in the presence of heparin (1 μg/mL), and reactions were started with 6 different concentrations of S2222 (not shown). Figure 5C shows the plot of the IC_{50} values and S2222 concentrations; fitting with linear regression determined a noncompetitive type of inhibition with K_i 7.85 ± 1.07 nM. The effects of heparin were tested in FXIa inhibition using S2366. Figure 5D shows that heparin at concentrations as low as 0.1 μg/mL enhances FXIa inhibition by Desmolaris; Figure 5E depicts a dose-dependent inhibition curve. Next, Desmolaris was incubated with FXIa in the presence of heparin (1 μg/mL), and reactions were started with different concentrations of S2366 (not shown). Figure 5F shows the plot of the IC_{50} values and S2366 concentrations; fitting by linear regression determined a noncompetitive type of inhibition with K_i 0.97 ± 0.18 nM.

Figure 5G shows that dextran sulfate (DS) 500K, DS50K, heparin grade I, and heparan sulfate interact with Desmolaris. Experiments determined *KD* 76.96 ± 2.3 nM for heparin, according to resonance values obtained at steady state (Figure 5H; inset, sensorgrams) and *KD* 305.3 ± 19.7 nM for heparan sulfate (steady-state kinetics) (Figure 5I; inset, sensorgrams). In another experiment, Desmolaris was loaded in a heparin-agarose column followed by elution with a salt gradient. Figure 5J shows that Desmolaris is eluted with ~1 M NaCl, compatible with a high-affinity interaction.

Functional domains of Desmolaris

Figure 6A depicts a schematic representation of truncated forms of Desmolaris expressed in HEK293 cells; Figure 6B shows the sodium dodecyl sulfate-polyacrylamide gel electrophoresis (SDS-PAGE) for all purified forms. The effects of Desmolaris truncated forms and

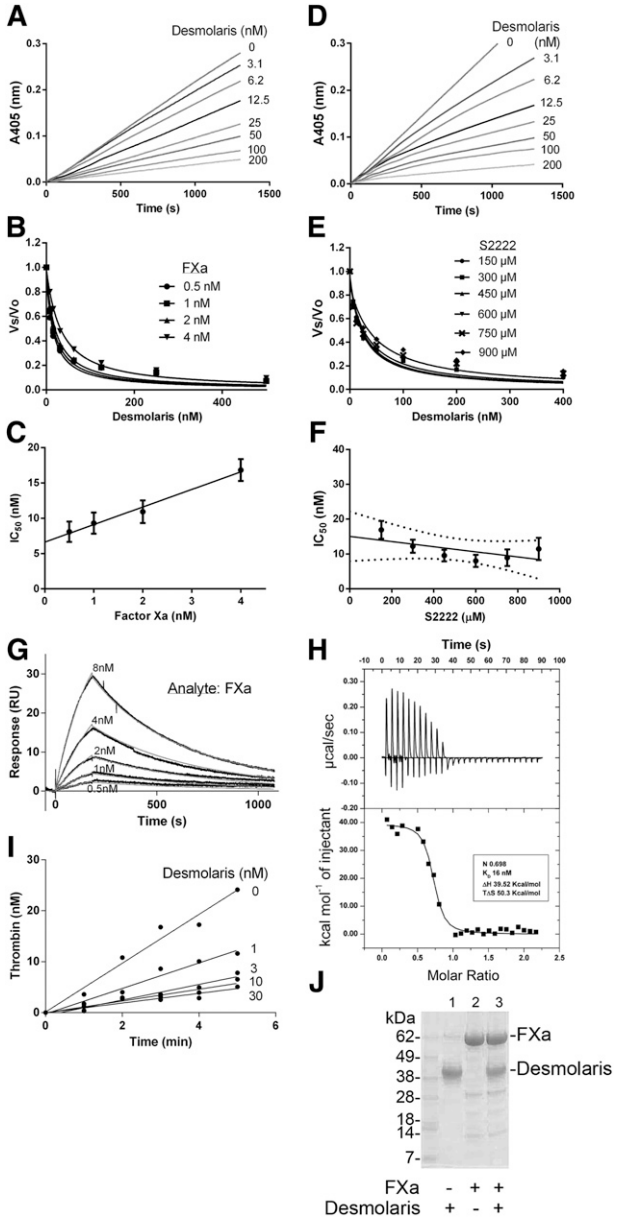

Figure 3. Desmolaris is a slow and tight inhibitor of FXa. (A) Inhibition of the catalytic activity of FXa. Reactions started with addition of S2222 (250 μM) to a mixture containing Desmolaris incubated for 1 hour with FXa (1 nM). Substrate hydrolysis was followed for 2 hours at 405 nm. (B) Tight inhibition. Experiments were performed as in (A) but at 0.5, 1, 2, and 4 nM FXa. The rate of substrate hydrolysis between 30 and 60 minutes (*Vmax* mode) was transformed as *Vs*/*Vo* and plotted against Desmolaris concentration. Data points were fitted with the Morrison equation to calculate the IC_{50} at each enzyme concentration. (C) Plot of IC_{50} and FXa produces a straight line typical of tight inhibitors. (D) Slow-type inhibition. Reactions started with addition of FXa (1 nM) to a mixture containing Desmolaris and S2222 (250 μM). Substrate hydrolysis was followed for 2 hours at 405 nm. (E) IC_{50} determination. FXa was added to Desmolaris in the presence of S2222 (150, 300, 450, 600, 750, and 900 μM). The ratio *Vs*/*Vo* obtained (*Vmax* mode) between 30 and 60 minutes was plotted against S2222 concentrations. Data were fitted with the Morrison equation to calculate the IC_{50} values at each substrate concentration. Six experiments were performed, and each data point is the average of duplicate determinations. (F) Determination of the K_i. Plot of IC_{50} vs S2222 concentrations was fitted by linear regression and the *y* intercept equals the K_i. Confidence interval is shown as dotted lines. (G) SPR experiments. Factor Xa at the indicated concentrations was injected over immobilized Desmolaris for 180 seconds. Dissociation of the Desmolaris-FXa complex was monitored for 900 seconds. Representative sensorgrams are shown in black lines; global fitting of the data points using the Langmuir equation is depicted in red lines. (H) Solution binding of Desmolaris to FXa by ITC. (Upper panel) Baseline-adjusted heats per injection of FXa (10 μM) into Desmolaris (1.0 μM). (Lower panel) Molar enthalpies per injection for FXa

variants in FXa and FXIa amidolytic activity were determined using S2222 or S2366, respectively. Reactions were started by adding the chromogenic substrate to a mixture containing FXa or FXIa and Desmolaris forms. Figure 6C-D shows that Desmolaris promotes inhibition of FXa and FXIa with an IC_{50} of 1.49 ± 0.34 nM and 1.32 ± 0.09 nM, respectively. In contrast, K1K2 (Desmolaris containing the amino-terminal, Kunitz-1, linker, and Kunitz-2) inhibits FXa with an IC_{50} of 7.13 ± 0.72 nM, and FXIa with IC_{50} 48.21 ± 4.11 nM. K1 (the N terminus, Kunitz-1, and linker) was active with IC_{50} 50.06 ± 4.5 nM for FXa and 11.2 ± 1.74 nM for FXIa. R32L, K2Long (Kunitz-2 and C terminus), and K2Short (Kunitz-2 only) were mostly inactive for FXa (Figure 6C) and FXIa (Figure 6D). Figure 6E-F confirms that Desmolaris interferes with the PT and aPTT. Although K1K2 prolongs twofold the PT at 1 μM, it remarkably prolonged the aPTT at 300 nM. In addition, K1 slightly affected the aPTT at 300 nM, but was without effect in the PT, at 1 μM. All other forms (up to 1 μM) were inactive in both coagulation assays (not shown).

Figure 6G-H shows that inhibition of both enzymes by K1K2 was dramatically enhanced by heparin, with curves similar to Desmolaris. Inhibition of the enzymes by "K1" was not potentiated by heparin. Because the other forms did not affect the amidolytic activity of the enzymes, they were not tested in the presence of heparin. Next, each form was loaded in a heparin-agarose column and the concentration of salt needed for elution was used as an estimate of relative affinity. Figure 6I shows the following affinity for heparin-agarose gel: Desmolaris = R32L = K2Long > K2Short > K1K2. In contrast, "K1" did not bind to a heparin-agarose column. The putative targets for each domain of Desmolaris are shown in Figure 6J.

Anti-inflammatory and antithrombotic effects of Desmolaris

To test whether Desmolaris display antithrombotic activity, $FeCl_3$ was used to induce carotid artery injury.[26] Thrombus formation was estimated using a Doppler flow probe. Times to occlusion were not significantly different between control (18.10 ± 1.3 minutes) and mice treated with 10 μg/kg Desmolaris (21.4 ± 5.2 minutes); however, all mice treated with 100 μg/kg Desmolaris were resistant to arterial occlusion, which did not take place before 60 minutes for all animals (Figure 7A). The effects of Desmolaris in bleeding were estimated using the tail transection method and the hemoglobin content at 540 nm. Desmolaris (100 μg/kg or 250 μg/kg) did not produce bleeding, which was significant only at higher doses (>250 μg/kg; Figure 7B). Then, plasma from mice injected with the anticoagulant were collected and used for determination of PT and aPTT ex vivo. Desmolaris at 250 μg/kg prolongs the aPTT but does not affect the PT (Figure 7C). This is compatible with an inhibitor targeting the contact pathway.

The finding that Desmolaris inhibits kallikrein suggests that the inhibitor might attenuate inflammation triggered by activation of

Figure 3 (continued) interaction with Desmolaris. Filled squares, measured enthalpies; solid line, fit of experimental data to a single site-binding model. Thermodynamic parameters: ΔH in kcal/mol, TΔS in kcal/mol, and *KD* are indicated in the inset. (I) Effects of Desmolaris in the prothrombinase complex. FXa was incubated with Desmolaris (0-30 nM) followed by addition of FVa, phosphatidylcholine/phosphatidylserine, and prothrombin in the presence of Ca^{2+}. Aliquots were taken to estimate thrombin generation. Data points are the average for triplicate determination. (J) Cleavage of Desmolaris. Desmolaris (7.5 μM) was incubated with FXa (1.7 μM) for 8 hours. The mixture was loaded in a NuPAGE gel. The bands corresponding to FXa or Desmolaris are indicated. Lane 1, Desmolaris; lane 2, FXa; lane 3, FXa plus Desmolaris. No cleavage is observed.

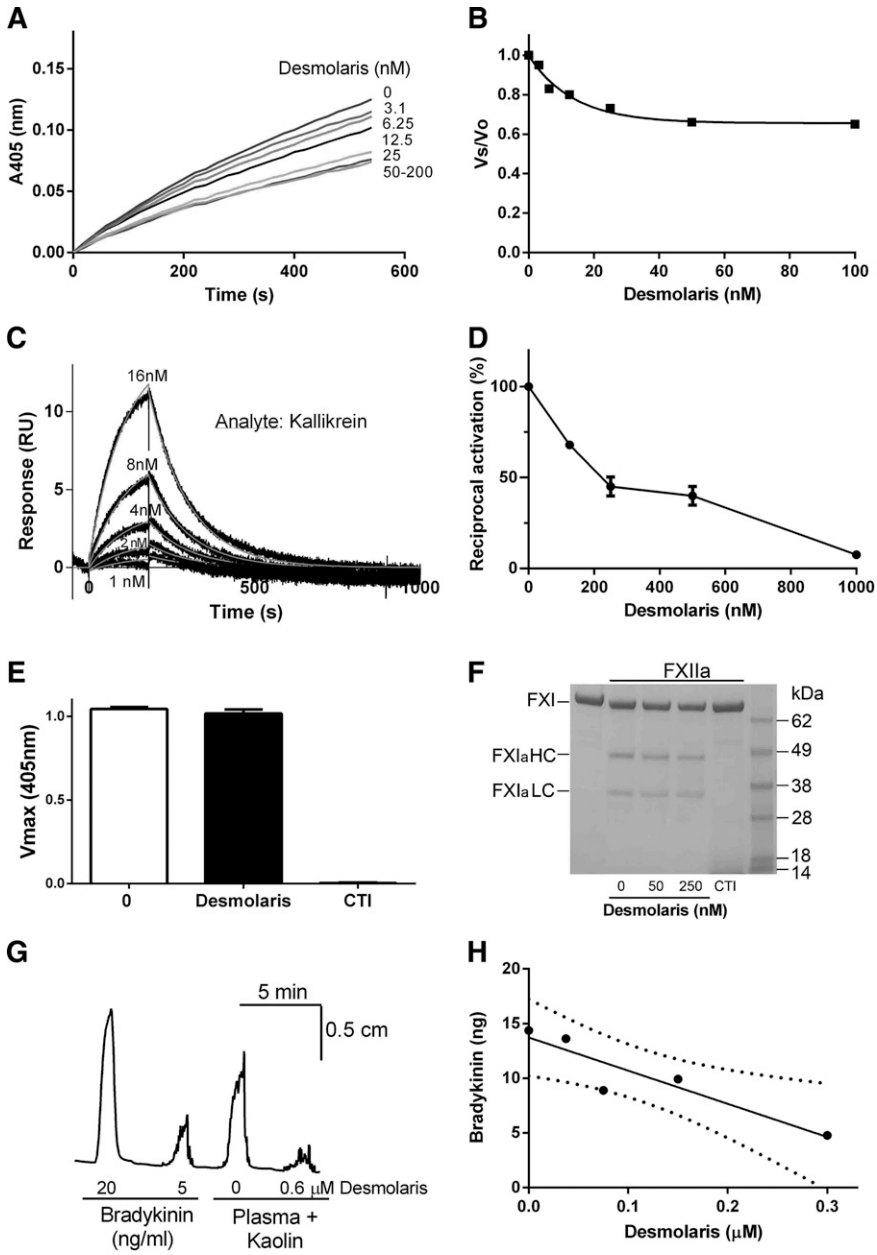

Figure 4. Desmolaris inhibits kallikrein, but not FXIIa. (A) Inhibition of the catalytic site of Kallikrein. Reactions started with addition of S2302 (250 μM) to a mixture containing Desmolaris incubated for 1 hour with Kallikrein (2 nM). Substrate hydrolysis was followed for 2 hours at 405 nm. (B) The ratio of *Vs*/*Vo* was plotted against Desmolaris concentration. (C) SPR experiments. Kallikrein at the indicated concentrations was injected over immobilized Desmolaris for 180 seconds. Dissociation was monitored for 900 seconds. Representative sensorgrams are shown in black lines; global fitting using the Langmuir equation is depicted in red lines. Representative experiment is shown. (D) Reciprocal activation. Factor XII (0.2 nM) was preincubated with Desmolaris (0, 62, 125, 250, 500, and 1000 nM) in 20 mM Tris, 0.15 M NaCl, 0.3% bovine serum albumin, pH 7.4, for 10 minutes at room temperature. Reactions were started by addition of PK (10 nM) and DS 500 (0.2 μg/mL, final concentrations). After 10 minutes, S2302 (250 μM) was used as substrate. Each data point is the mean ± standard error of a triplicate determination. (E) Desmolaris does not inhibit the amidolytic activity of FXIIa. FXIIa (2 nM) was incubated with Desmolaris (50 nM) for 15 minutes, followed by addition of S2302 (250 μM). Substrate hydrolysis was followed for 1 hour at 405 nm. No inhibition was observed. CTI (5 μM) was used as a control inhibitor. (F) Desmolaris does not inhibit FXI activation by FXIIa. FXIIa (25 nM) was incubated with Desmolaris (0, 50, and 250 nM) in Tris-buffered saline for 20 minutes followed by addition of FXI (100 μg/mL). After 8 hours at 37°C, reactions were stopped with reducing SDS sample buffer and samples loaded in 4% to 12% NuPAGE gel. FXIa HC and FXIa LC were visualized in Coomassie Blue-stained gels. CTI (5 μM) was used as control inhibitor. A representative gel is shown. (G) BK formation in plasma. Coagulation activation by the contact pathway was activated by kaolin (to generate BK) in the presence of PBS or 0.6 μM Desmolaris. The mixture was transferred to a chamber containing a guinea-pig ileum, which is responsive to BK. As a control, BK (5 and 20 ng/mL, final concentrations) was added directly to the ileum. (H) Dose-response curve for experiments depicted in panel G. Each data point is the mean ± standard error of a triplicate determination. Confidence interval is shown as dotted lines. IC_{50} value for inhibition of BK formation is ~200 nM.

the contact pathway.[4,5] For example, polyPs, which activate FXII, induce an increase in vascular permeability that can be estimated with the Miles assay of fluid extravasation to the skin using Evans blue.[31] Figure 7D shows that polyPs promote intense extravasation (positive control). In contrast, Desmolaris (500 μg/kg) prevented this response almost completely, similar to PBS (negative control). Figure 7E shows the quantification of these results.

FXa induces a transient paw edema formation in rats or mice through PAR2 activation.[32] Figure 7F shows that, in the presence of Desmolaris, edema formation is reduced, implying that it blocks FXa activity in vivo. After injecting a mixture containing collagen plus epinephrine into the cava vein of mice, activation of platelets and coagulation results in thromboembolism and occlusion of pulmonary vessels.[10,31,33] As a result, respiratory distress and death of most animals takes place within 5 minutes (Figure 7G). Although Desmolaris at 100 μg/kg did not affect survival (not shown), 500 μg/kg or 1 mg/kg produced dose-dependent protection with up to 40% of animals surviving at the highest dose of the inhibitor. Histological sections of the lungs confirmed the presence of thrombi, which were remarkably reduced in animals treated with Desmolaris (1 mg/kg) (Figure 7H).

Discussion

The presence of anticoagulant activity in vampire bat saliva was initially suggested in 1932.[18] However, the molecular identity of the coagulation inhibitor remained elusive. More recently, the first transcriptome analysis of the principal submaxillary gland of *D. rotundus* was reported.[22] This extensive database identified—among several genes—1 candidate member of the Kunitz family of proteins that was annotated as an anticoagulant based on its similarity to TFPI.[12,22]

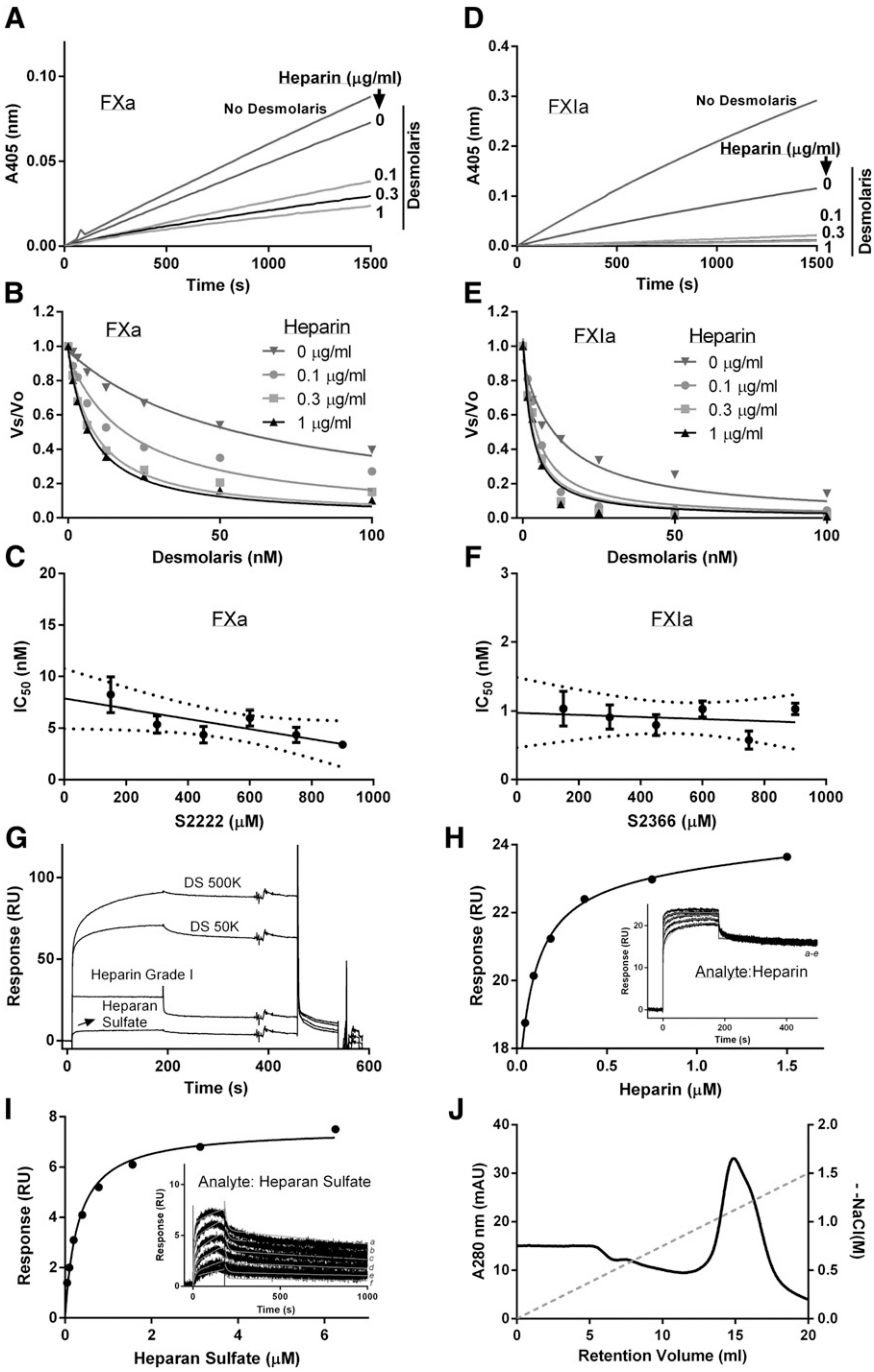

Figure 5. Heparin is a cofactor for Desmolaris. (A) Inhibition of catalytic activity of FXa. Reactions started with addition of S2222 (250 μM) to a mixture containing FXa (0.5 nM), Desmolaris (25 nM), and heparin (0, 0.1, 0.3, and 1 μg/mL) preincubated for 1 hour. Substrate hydrolysis was followed for 2 hours at 405 nm. (B) The experiment was performed as in (A) but at the indicated concentrations of Desmolaris and heparin. The ratio of *Vs*/*Vo* was plotted against Desmolaris concentration and data fitted with the Morrison equation. (C) Determination of the K_i in the presence of heparin. The IC_{50} value for inhibition of FXa (0.5 nM) by Desmolaris (0-100 nM), in the presence of 1 μg/mL heparin was determined for each S2222 concentration (150, 300, 450, 600, and 750 μM) (not shown). Reactions were started with FXa. The plot of IC_{50} and S2222 was fitted by linear regression and the K_i was determined by the *y* intercept. Six experiments were performed, and each data point is the average of duplicate determinations. (D) Inhibition of catalytic activity of FXIa. Reactions started with addition of S2366 (250 μM) to a mixture containing FXIa (0.5 nM), Desmolaris (12.5 nM), and heparin (0, 0.1, 0.3 and 1 μg/mL) preincubated for 1 hour. Substrate hydrolysis was followed for 2 hours at 405 nm. (E) The experiment was performed as in panel D but at the indicated concentrations of Desmolaris and heparin. The ratio of *Vs*/*Vo* was plotted against Desmolaris concentration and data fitted with the Morrison equation. (F) Determination of the K_i in the presence of heparin. The IC_{50} for inhibition of FXIa (0.5 nM) by Desmolaris (0-100 nM), in the presence of 1 μg/mL heparin was determined for each S2366 concentration (150, 300, 450, 600, and 750 μM) (not shown). Reactions were started with FXIa. The plot of IC_{50} and S2366 was fitted by linear regression and the K_i was determined by the *y* intercept. Six experiments were performed, and each data point is the average of duplicate determinations. (G) Binding of heparin and dextran sulfate. Desmolaris was immobilized in a CM5 sensor chip followed by injection of DS500K (200 nM), DS50K (200 nM), heparin Grade I (40 μM), or heparan sulfate (8 μM). All analytes were diluted in HEPES-buffered saline Tween (0.05% v/v) (HBS-P). (H) Heparin binding to Desmolaris. Heparin concentrations indicated in the inset: (*a*) 1.5 μM, (*b*) 0.75 μM, (*c*) 0.375 μM, (*d*) 0.187 μM, (*e*) 0.093 μM, and (*f*) 0.0.046 μM were injected over immobilized Desmolaris. The values obtained at equilibrium binding (steady state) were used to determine the *KD*. A representative experiment is shown. (I) Heparan sulfate binding to Desmolaris. Heparan sulfate concentrations indicated in the inset: (*a*) 6.25 μM, (*b*) 3.13 μM, (*c*) 1.5 μM, (*d*) 0.75 μM, (*e*) 0.3 μM, and (*f*) 0.15 μM were injected over immobilized Desmolaris. The values obtained at equilibrium binding (steady state) were used to determine the *KD*. A representative experiment is shown. (J) Desmolaris interacts with a heparin-agarose column. Desmolaris (200 μL; 20 μM) was added to the heparin column and equilibrated in TBS, pH 7.4. After washing the column, a gradient (NaCl, 0-2 M) was applied for 40 minutes. The peak corresponding to Desmolaris eluted at ~1 M NaCl. *mAU*, milliabsorbance units. Representative experiments are shown.

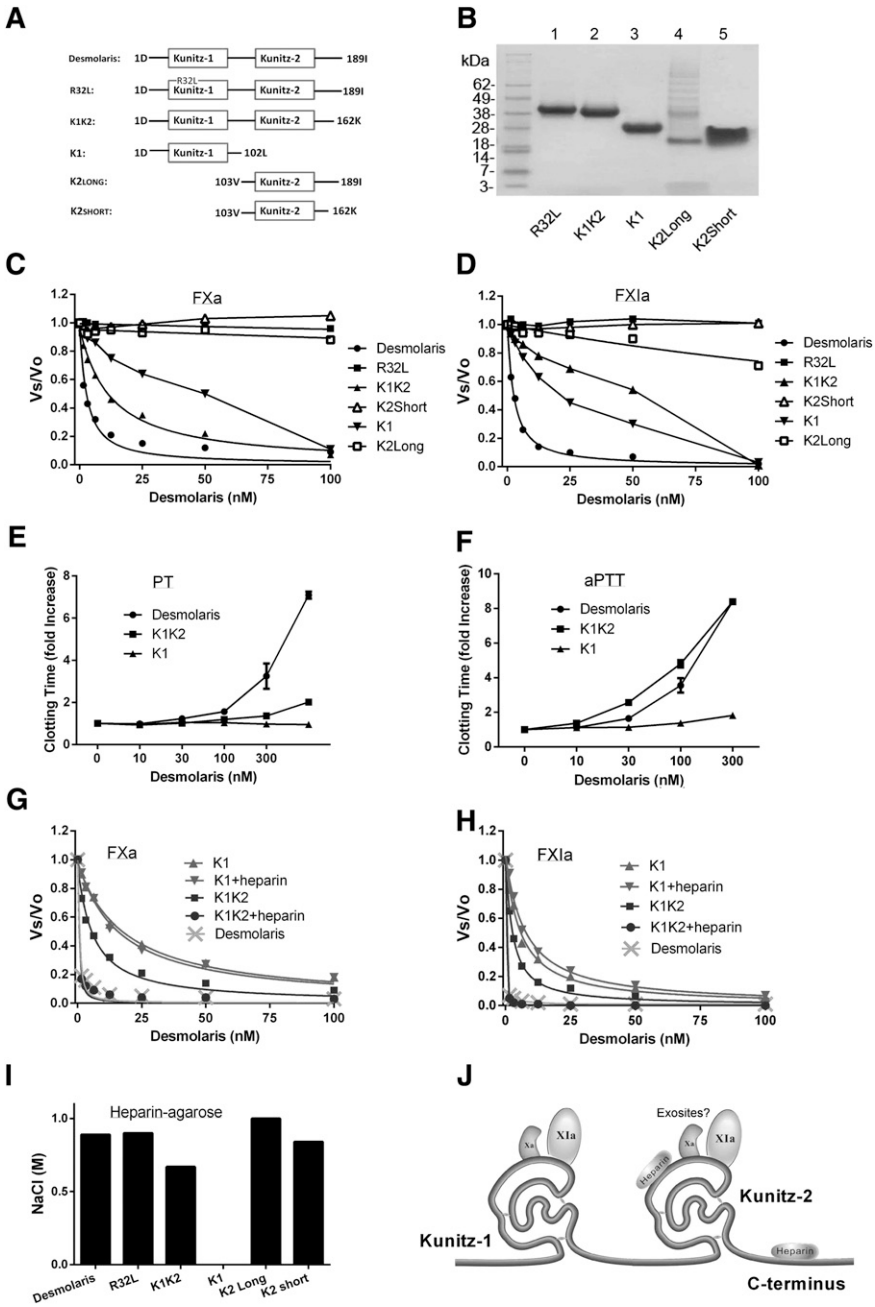

Figure 6. Functional domains of Desmolaris. (A) Domain representation for Desmolaris. All truncated forms were designed based on sites of introns determined for TFPI,[12] as indicated in Figure 1B. (B) SDS-PAGE of the mutated and truncated forms of Desmolaris. Gels were Coomassie Blue-stained. Lane 1, R32L; lane 2, K1K2; lane 3, K1; lane 4, K2Long; lane 5, K2Short. (C) Effects on the catalytic activity of FXa. FXa (1 nM) was incubated for 30 minutes with the indicated forms of Desmolaris followed by addition of S2222 (250 μM). The ratio *Vs*/*Vo* obtained was plotted against Desmolaris concentration and data fitted (when appropriate) with the Morrison equation to calculate the IC_{50} for each form. (D) Effects on the catalytic activity of FXIa. FXIa (1 nM) was incubated for 30 minutes with the indicated forms of Desmolaris followed by addition of S2366 (250 μM). The ratio *Vs*/*Vo* obtained was plotted against Desmolaris concentration and data fitted (when appropriate) with the Morrison equation to calculate the IC_{50} for each form. (E) Effects on the PT. Desmolaris forms were incubated with plasma followed by addition of PT reagent and Ca^{2+}. Clotting was estimated with a coagulometer. Reference time is 14.6 seconds. (F) Effects on the aPTT. Desmolaris forms were incubated with plasma followed by addition of aPTT reagent and Ca^{2+}. Clotting was estimated with a coagulometer. Reference time was 35.9 seconds. (G) Effects of heparin on FXa inhibition by K1 and K1K2. Comparison with Desmolaris. Experiments were performed as in panel C in the absence or presence of heparin (1 μg/mL) and the indicated concentrations of Desmolaris forms. FXa, 0.5 nM. Data points were fitted with Morrison equation. (H) Effects of heparin on FXIa inhibition by K1 and K1K2. Comparison with Desmolaris. Experiments were performed as in panel D in the absence or presence of heparin (1 μg/mL) and the indicated concentrations of Desmolaris forms. FXIa, 0.5 nM. Data points were fitted with Morrison equation. (I) Interaction of Desmolaris forms with a heparin-agarose column. Desmolaris, R32L, K1K2, K1, K2Long, or K2Short were loaded in the heparin column and equilibrated in TBS, pH 7.4. A total of 200 μL of each form at ~20 μM were applied. After washing the column, a gradient (NaCl, 0-2 M) was applied for 40 minutes. The peak corresponding to Desmolaris eluted at ~1 M NaCl. (J) Diagram of the putative interactions of Desmolaris domains with FXa, FXIa, and heparin. ?, putative interactions with exosites of FXIa or FXa.

Analysis of this sequence, which codes for a protein named Desmolaris, indicated that it contains, similarly to TFPI, a basic carboxyl-terminal (C-terminal) that confers binding to heparin[34] and optimal inhibition of FXa.[35] In contrast, Desmolaris presents a natural deletion of the Kunitz-1 domain of TFPI that mediates interaction with FVIIa/TF.[23] Compatible with the deletion, Desmolaris does not block FVIIa/TF. Sequence alignment also revealed that the Kunitz-1 and -2 of Desmolaris correspond, respectively, to the Kunitz-2 and -3 of TFPI. Furthermore, the corresponding Kunitz-1 and -2 of both inhibitors are highly homologous and display positively charged arginine in the P_1 position that, in TFPI, mediates FXa inhibition.[23] On the other hand, Desmolaris Kunitz-2 exhibits asparagine in the P_1 position, which is arginine in the Kunitz-3 of TFPI, that interact with Protein S.[29,30] Moreover, several highly conserved residues present in the Kunitz-3 of TFPI family members were found to be replaced by amino acids of different chemical class in the Kunitz-2 of Desmolaris.

Deletion of a Kunitz domain and other substitutions observed in the Kunitz-2 of Desmolaris suggested that an important gain of function took place evolutionarily. Accordingly, we discovered that Desmolaris, contrarily to TFPI, is a slow, tight, and noncompetitive inhibitor of FXIa (K_i 12.35 nM) with respect to S2366. These experiments determine the mode of inhibition and relative affinity of the inhibitor for the catalytic site of the enzyme with respect to the small chromogenic substrate. However, SPR experiments—which evaluate macromolecular interactions beyond the catalytic site—estimated a much tighter *KD* (picomolar range). Our interpretation is that exosites play a major role in enzyme-inhibitor complex formation. Together with a noncompetitive type of inhibition, this explains why *Ki* and *KD* are not congruent. Kinetic calculation of the *KD* by SPR using the ratio

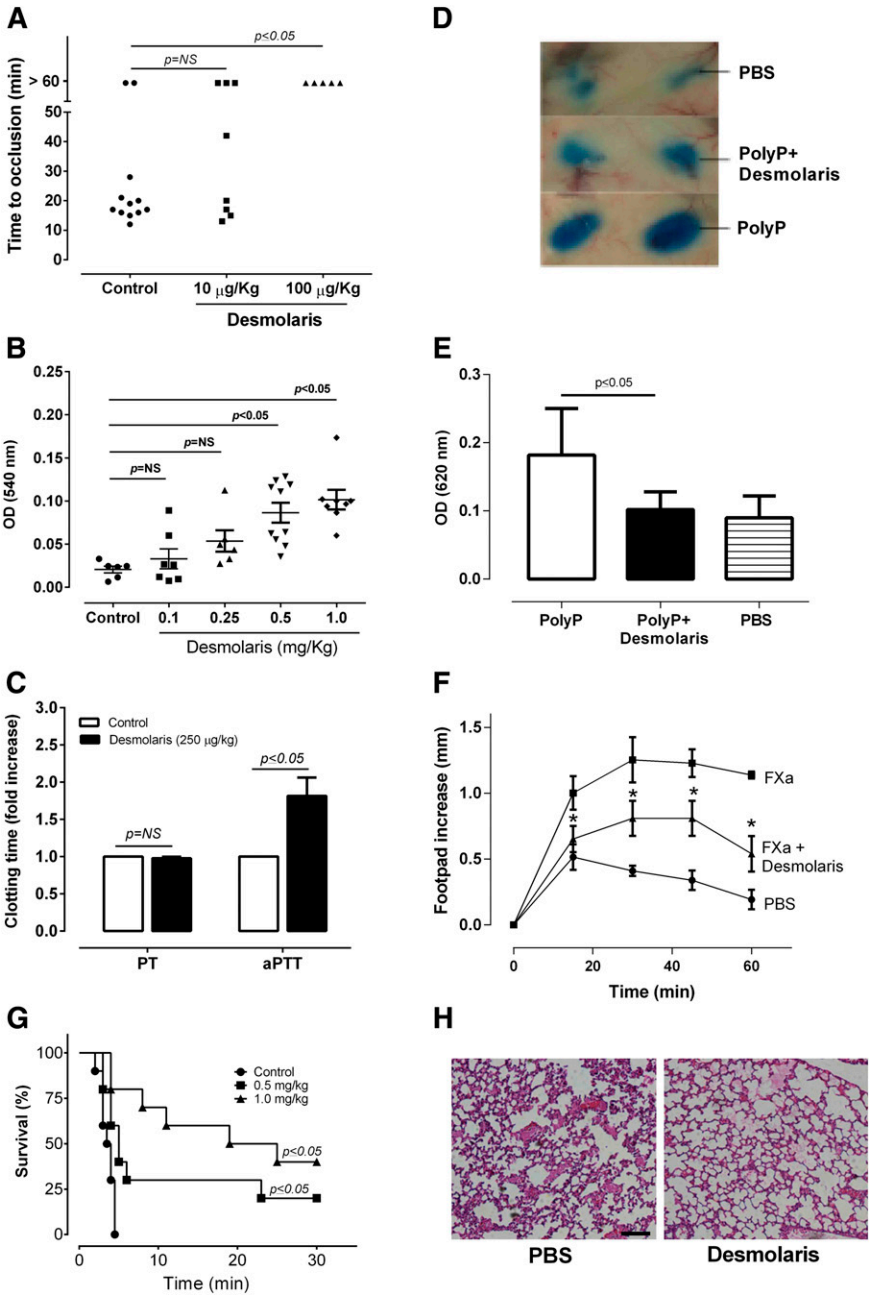

Figure 7. Anti-inflammatory and antithrombotic activity of Desmolaris. (A) Thrombosis. A paper filter imbibed with 7.5% $FeCl_3$ was applied to the carotid artery, and blood flow was monitored with a perivascular flow probe for 60 minutes or until stable occlusion took place. Fifteen minutes before injury, Desmolaris was injected into the caudal veins of the mice. Each symbol represents one individual. $^*P < .05$ (analysis of variance [ANOVA] with Dunnett posttest). (B) Bleeding time. Bleeding was caused by a tail transection after IV infection of Desmolaris as the indicated concentrations. Absorbance at 540 nm (hemoglobin concentration) was used to estimate blood loss. $^*P < .05$ (ANOVA with Dunnett posttest). (C) aPTT and PT ex vivo. The aPTT or PT reagents were added to plasma collected from mice injected with Desmolaris (250 μg/kg) or PBS (control). Clot was determined using a coagulometer (n = 6; $^*P < .05$; *t* test; NS, nonsignificant). The ratio of clotting times is shown. Absolute values: PT; 11.67 ± 0.33 seconds; aPTT, 49.99± 4 seconds. (D) Vascular permeability (Miles assay). A total of 100 μL of a mixture containing Evan's blue and Desmolaris (500 μg/kg) was injected IV into the tails of mice. Five minutes later, 40 μL of polyphosphate (polyP; 0.2 mg/mL) was injected intradermally. After 20 minutes, animals were sacrificed and skin removed to allow sites of injection to be photographed. (E) Evans blue extravasation was estimated after extraction with formamide and reading at 620 nm. Results are the average of experiments obtained with 4 animals for each condition. $^*P < .05$ (ANOVA). (F) Desmolaris blocks the inflammatory effects of FXa. Posterior paw edema was induced by intradermal injection of 30 μL of FXa (10 μg, 7.3 μM) in the presence of PBS (squares), or FXa previously incubated with 10 μM of Desmolaris (triangles). Edema caused by 30 μL of PBS only is shown by circles. Edema formation (increase in paw thickness in millimeters) was estimated with a caliper before injection of FXa or after 15, 30, 45, and 60 minutes. Four posterior paws were used for each data point. $^*P < .05$ (ANOVA). (G) Kaplan-Meier survival curves. Mortality associated with thromboembolism triggered by an IV injection of collagen (0.8 mg/kg) and epinephrine (60 μg/kg) after administration of either PBS (control) or Desmolaris. Animals that were alive 30 minutes after the challenge were considered to be survivors. Each symbol represents one individual. $^*P < .05$ (log-rank test). (H) Histology of the lung. Hematoxylin and eosin-stained lung sections of control (PBS) and Desmolaris-treated (1000 μg/kg) mice. Animals were euthanized 5 minutes after collagen and epinephrine injection. Representative images from 3 animals for each condition. Bars represent 100 μm.

koff/*kon* was not possible because of the very slow dissociation rate, which approached the limits that can be measured by the instrument. To circumvent this limitation, SPR experiments were performed in which the affinity for FXIa/Desmolaris complex was determined by equilibrium binding (*KD* 0.63 nM). ITC experiments also confirmed that enzyme and inhibitor interact in solution and revealed that approximately 2 Desmolaris molecules bind 1 FXIa, a result compatible with the enzyme being dimeric.[28] However, accurate determination of the *KD* was not possible with ITC because of the tight nature of the inhibitor. In these cases, as observed here, the titration curves have a typical pattern because the value for *c* exceeds 1000, as reviewed elsewhere.[27] Nonetheless, assuming *KD* ~0.5 nM, it is concluded that Desmolaris inhibits FXIa with an affinity at least 30 times higher than calculated for other enzymes (eg, FXa). Moreover, concentrations of FXIa around the *KD* would conceivably be inhibited by Desmolaris, in vivo.

Interaction of Desmolaris with FXIa was also found to be functionally relevant because it prevented FIX activation by FXIa and caused a profound prolongation of the aPTT relative to PT. Interestingly, this marked effect in the aPTT has been observed before with vampire bat saliva, suggesting that Desmolaris accounts for this activity in nature.[19] Whether other molecules identified in the transcriptome analysis of the gland[22] contribute to the anticoagulant activity of saliva remains to be determined. Experiments also demonstrated that inhibition of FXIa by Desmolaris was enhanced 12 times by heparin. This implies that the glycosaminoglycan functions as a cofactor, possibly through a template or allosteric mechanisms involving basic residues of the inhibitor and the heparin-binding sites of the enzyme.[28,36] Furthermore, binding of Desmolaris to heparin was confirmed by SPR and by using a heparin-agarose column. It is plausible that glycosaminoglycans are important to localize Desmolaris at the vascular endothelium, which is rich in heparan sulfate.[12]

Consistent with similarities to the Kunitz-2 of TFPI, Desmolaris was identified as a slow, tight, and noncompetitive inhibitor of FXa (K_i 15 nM) with respect to S2222. ITC experiments determined that the reaction in solution is stoichiometric (1:1) with a *KD* of 16 nM; this value is in excellent agreement with the *KD* of 17 nM calculated by SPR. Desmolaris interacts with mice FXa with similar affinity. Inhibition of FXa was functionally characterized by attenuation of the prothrombinase complex in reactions initiated by addition of prothrombin to FXa/Desmolaris but not when started with prothrombin/Desmolaris. These results imply that Desmolaris, like physiologic concentrations of TFPI, preferentially inhibits free FXa but not FXa assembled in the prothrombinase complex.[37] In regard to cofactor requirements, inhibition of FXa by Desmolaris was only slightly (2 times) increased by heparin, which in the case of TFPI is significantly enhanced.[34] On the other hand, Protein S—a cofactor for FXa inhibition by TFPI[29,30]—did not affect inhibition by Desmolaris (not shown). Structural features present in the Kunitz-3 domain of TFPI but absent in Desmolaris might explain the distinct cofactor dependency of both inhibitors.

The activity of Desmolaris toward FXIa resembles the specificity of protease nexin-2 (PN2, Alzheimer β-amyloid protein precursor), a Kunitz-type inhibitor of FXIa (K_i ~0.5 nM), released by activated platelets.[38] Of note, the anticoagulant activity for PN2 resides in the Kunitz domain (PN2KPI).[39] Interestingly, PN2KPI aligns better with Kunitz-2 of Desmolaris (not shown), suggesting that this domain might mediate—at least in part—FXIa inhibition. To determine how Desmolaris interacts with FXIa, FXa, and heparin, a series of truncated forms and 1 variant of the P_1 position (R32L) were expressed. Experiments with R32L determined that Arg32 in the Kunitz-1 is the residue involved in the interaction of Desmolaris with catalytic sites of enzymes. Kunitz-2, based on results with K1K2, is suggested to have an accessory role, possibly by stabilizing Desmolaris in the right conformation or through direct interaction with FXIa and FXa. It is also clear from results with K1K2 that the C-terminal is required for optimal inhibition of FXa and FXIa by Desmolaris, as reported for TFPI.[35] Experiments with K1K2 also revealed that Kunitz-2 is required for enhancement of FXIa and FXa inhibition by Desmolaris in the presence of heparin, this interaction being optimized by the C terminus domain. Furthermore, experiments with K2Short and K2Long provided direct evidence that Kunitz-2 and the C-terminal domain of Desmolaris mediate interaction with heparin, a property reminiscent of TFPI.[34] In agreement with the results with chromogenic substrate, K1K2 and to a much lesser extent K1 were the only forms that affected the PT and particularly the aPTT. Altogether, Desmolaris has lost the ability to interact with FVIIa/TF and PS, described for TFPI; notably, however, it became a potent inhibitor of FXIa. These results highlight the remarkable plasticity of Kunitz family of proteins and identify a unique specificity for a novel member of the TFPI family of anticoagulants.

In the contact pathway, FXII activation is initiated by negatively charged molecules.[5,40] No evidence for inhibition of FXIIa by Desmolaris was obtained with 2 independent methods. After activation, FXIIa converts PK to kallikrein that cleaves HMWK and generates BK, which produces pain and increases vascular permeability.[5] Desmolaris was found to interact with kallikrein and to partially inhibit its amidolytic activity. As a result, Desmolaris abrogated the reciprocal activation of FXII and PK in vitro and effectively attenuated BK formation in plasma activated with kaolin. Evidence for kallikrein inhibition by Desmolaris in vivo was provided by experiments using intradermal injections of polyPs (Miles assay).[31] These results showed less extravasation of Evan's blue, indicating inhibition of BK formation. This discovery is relevant because BK displays pro-inflammatory functions through BK receptors and therefore contributes to inflammation associated with thrombosis, particularly in stroke models.[41] Accordingly, interaction of Desmolaris with FXIa and kallikrein provides effective anticoagulation by inhibition of the consolidation phase of the coagulation cascade on the 1 hand[1] and attenuation of the pro-inflammatory component of the contact pathway[41] on the other. Screening assays also determined that Desmolaris inhibits neutrophil elastase, an enzyme that contributes to thrombotic events.[42] The significance of this interaction remains to be evaluated.

Ferric chloride–induced carotid thrombus formation in mice was used to test the antithrombotic properties of Desmolaris.[43] Results demonstrated that Desmolaris completely inhibited arterial thrombosis at 100 μg/kg. Notably, at this concentration and higher (250 μg/kg), no significant bleeding was observed. Therefore, it is conceivable that FXIa is the main target in vivo for Desmolaris, when tested at antithrombotic concentrations. This assumption is based on (1) the highest affinity for FXIa vs other coagulation factors, as calculated by SPR, ITC, and kinetics experiments; (2) the prolongation of the aPTT ex vivo without change in the PT; (3) the finding that salivary inhibitors targeting FXa (eg, tick anticoagulant peptide, antistasin, Lufaxin),[26,44] but not FIX(a) (eg, nitrophorin-2),[45] inhibit experimental thrombosis at concentrations that consistently promote bleeding; and (4) the emerging concept that FXIa plays a major role in thrombus formation in vivo but not for hemostasis.[11,46] Accordingly, interference with FXI(a) function through genetic deletion,[43,46] blockade with antibodies[9,10] or small-molecule inhibitors,[47] or by reduction of FXI synthesis with antisense oligonucleotides[48] results in inhibition of thrombosis with no bleeding phenotype. This profile, also observed here with Desmolaris, represents a novel antithrombotic strategy associated with potentially safe anticoagulation.[11,47] Nevertheless, Desmolaris may interfere with hemostasis at higher doses (>250 μg/kg), which is compatible with an anticoagulant targeting FXa. In fact, Desmolaris inhibits FXa-triggered paw edema in mice, an inflammatory event associated with PAR2 activation.[32] Blockade of FXa and FXIa by Desmolaris may also explain its protective effects in the thromboembolism model, which is partially dependent on coagulation activation.[10,31,33] Therefore, the concentrations of Desmolaris chosen for in vivo experiments should be critically evaluated in order to preferentially inhibit the contact vs the common pathway and to minimize bleeding.

Our results show that Desmolaris exhibits a distinct mechanism of action, enzyme specificity, and possibly pharmacokinetics compared with other relevant inhibitors of FXIa. For example, PN2KPI is a competitive inhibitor of FXIa, but a very weak inhibitor for FXa,[38,39] and prevents stroke without impairing hemostasis at plasma concentrations of 1-2 μM.[49] For comparison, Desmolaris at 100 μg/kg equals 2 μg per mouses (antithrombotic dose) and may reach a maximum theoretical blood concentration of 0.075 μM, assuming no losses and 1.5-mL volemia. Likewise, inhibition of thrombosis by Desmolaris occurs at concentrations 10 times lower than those observed with antibodies against FXI(a) (14E11 or aFXI, 1 mg/kg).[8,41] Desmolaris is also distinct to Ir-CPI, a Kunitz-type inhibitor from tick salivary glands that targets the exosite of FXIIa in addition to FXIa and kallikrein and prevents venous or arterial thrombosis at 1 mg/kg.[33] Moreover, Desmolaris differs from infestin-4, a Kazal-type inhibitor from insect midgut that inhibits FXIIa and blocks $FeCl_3$-induced mesenteric or carotid thrombosis at 20 mg/kg.[50] Other promising alternatives such as antisense oligonucleotide-mediated knockdown of factor XI levels exhibits a relatively slow onset,[47,48] whereas immediate inhibition

would be achieved with Desmolaris. Furthermore, plasma or FXI may overcome the anticoagulant activity of Desmolaris, in case of bleeding.[8,41] Desmolaris is not cleaved by FXa or FXIa, suggesting that it retains inhibitory activity after interaction with the enzymes.

Blockade of FXIa by Desmolaris is particularly important because it is the site of convergence for FXIIa- and thrombin-mediated contact pathway activation.[9-11,46] Therefore, Desmolaris emerges as a novel anticoagulant or prototype candidate for antithrombotic therapy in conditions associated with coagulation activation, particularly involving the contact pathway. Finally, the discovery of Desmolaris is historically relevant because it reveals the true identity of a major anticoagulant from the salivary gland of the vampire bat.

Acknowledgments

The authors thank Brenda Rae Marshall, DPSS, National Institute of Allergy and Infectious Diseases (NIAID), for editing, and Carl Hammer, Renee Olano, and Glenn Nardone (NIAID) for mass spectrometry analysis.

This work was supported by the Intramural Research Program of the Division of Intramural Research, NIAID, National Institutes of Health, and the Grant Agency of the Czech Republic (grant P502/12/2409) (M.K.).

Authorship

Contribution: D.M. provided experimental design, performed most in vitro experiments and Miles and paw edema assays, analyzed data, and contributed in writing; D.M.M. and R.Q.M. provided experimental design, performed experiments for thrombosis models and bleeding, analyzed data, and contributed with writing; T.C.F.A., Y.L., and Y.Q. performed experiments or analyzed data; J.M.C.R. and M.K. provided experimental design, performed experiments for bradykinin production or enzyme specificity, analyzed data, and contributed in writing; I.M.B.F. provided experimental design, performed experiments, analyzed data, and wrote the paper; all authors reviewed the final version of the manuscript.

Conflict-of-interest disclosure: The authors declare no competing financial interests. Because J.M.C.R. and I.M.B.F. are government employees and this is a government work, the work is in the public domain in the United States. Notwithstanding any other agreements, the National Institutes of Health reserves the right to provide the work to PubMedCentral for display and use by the public, and PubMedCentral may tag or modify the work consistent with its customary practices. You can establish rights outside of the United States subject to a government use license.

Correspondence: Ivo M. B. Francischetti, Section of Vector Biology, Laboratory of Malaria and Vector Research, NIAID/NIH, 12735 Twinbrook Parkway, Twinbrook III Bldg, Room 2E-32C, Rockville, MD 20852; e-mail: ifrancischetti@niaid.nih.gov.

References

1. Broze GJ Jr. Tissue factor pathway inhibitor and the revised theory of coagulation. *Annu Rev Med.* 1995;46:103-112.
2. Furie B, Furie BC. Mechanisms of thrombus formation. *N Engl J Med.* 2008;359(9):938-949.
3. Roberts HR, Monroe D III, Hoffman M. Molecular biology and biochemistry of the coagulation factors and pathways of hemostasis. In: Kaushansky K, Litchman MA, Beutler E, Kipps TJ, Seligsohn U, Prchal JT, eds. Williams Hematology. 8th ed. New York, NY: McGraw-Hill; 2010:1815-1844.
4. Renne T, Schmaier AH, Nickel KF, Blomback M, Maas C. In vivo roles of factor XII. *Blood.* 2012; 120(22):4296-4303.
5. Colman RW, Schmaier AH. Contact system: a vascular biology modulator with anticoagulant, profibrinolytic, antiadhesive, and proinflammatory attributes. *Blood.* 1997;90(10):3819-3843.
6. Walsh PN. Roles of platelets and factor XI in the initiation of blood coagulation by thrombin. *Thromb Haemost.* 2001;86(1):75-82.
7. Gailani D, Broze GJ Jr. Factor XI activation by thrombin and factor XIa. *Semin Thromb Hemost.* 1993;19(4):396-404.
8. Choi SH, Smith SA, Morrissey JH. Polyphosphate is a cofactor for the activation of factor XI by thrombin. *Blood.* 2011;118(26):6963-6970.
9. Gruber A, Hanson SR. Factor XI-dependence of surface- and tissue factor-initiated thrombus propagation in primates. *Blood.* 2003;102(3): 953-955.
10. Cheng Q, Tucker EI, Pine MS, et al. A role for factor XIIa-mediated factor XI activation in thrombus formation in vivo. *Blood.* 2010;116(19): 3981-3989.
11. Gailani D, Renne T. Intrinsic pathway of coagulation and arterial thrombosis. *Arterioscler Thromb Vasc Biol.* 2007;27(12):2507-2513.
12. Broze GJ Jr, Girard TJ. Tissue factor pathway inhibitor: structure-function. *Front Biosci.* 2012;17: 262-280.
13. Olson ST, Gettins PG. Regulation of proteases by protein inhibitors of the serpin superfamily. *Prog Mol Biol Transl Sci.* 2011;99:185-240.
14. Ribeiro JM, Francischetti IM. Role of arthropod saliva in blood feeding: sialome and post-sialome perspectives. *Annu Rev Entomol.* 2003;48:73-88.
15. Koh CY, Kini RM. Molecular diversity of anticoagulants from haematophagous animals. *Thromb Haemost.* 2009;102(3):437-453.
16. Francischetti IM, Valenzuela JG, Andersen JF, Mather TN, Ribeiro JM. Ixolaris, a novel recombinant tissue factor pathway inhibitor (TFPI) from the salivary gland of the tick, Ixodes scapularis: identification of factor X and factor Xa as scaffolds for the inhibition of factor VIIa/tissue factor complex. *Blood.* 2002;99(10):3602-3612.
17. Greenhall AM. Feeding behavior. In: Greenhall AM, Schmidt U, eds. Natural History of Vampire Bats. Boca Raton, FL: CRC Press; 1988:111-131.
18. Bier O. Action anticoagulante et fibrinolytique de l'extract de glandes salivaires d'une chauve-souris hematophage (Desmodus rufus). *CR Soc Biol (Paris).* 1932;110:129.
19. Hawkey CM. Salivary antihemostatic factors. In: Greenhall AM, Schmidt U, eds. Natural History of Vampire Bats. Boca Raton, FL: CRC Press; 1988: 133-142.
20. Apitz-Castro R, Beguin S, Tablante A, Bartoli F, Holt JC, Hemker HC. Purification and partial characterization of draculin, the anticoagulant factor present in the saliva of vampire bats (Desmodus rotundus). *Thromb Haemost.* 1995; 73(1):94-100.
21. Medcalf RL. Desmoteplase: discovery, insights and opportunities for ischaemic stroke. *Br J Pharmacol.* 2012;165(1):75-89.
22. Francischetti IM, Assumpcao TC, Ma D, et al. The "Vampirome": transcriptome and proteome analysis of the principal and accessory submaxillary glands of the vampire bat Desmodus rotundus, a vector of human rabies. *J Proteomics.* 2013;82:288-319.
23. Girard TJ, Warren LA, Novotny WF, et al. Functional significance of the Kunitz-type inhibitory domains of lipoprotein-associated coagulation inhibitor. *Nature.* 1989;338(6215): 518-520.
24. Williams JW, Morrison JF. The kinetics of reversible tight-binding inhibition. *Methods Enzymol.* 1979;63:437-467.
25. Copeland RA. Tight binding inhibitors. In: Copeland RA. Enzymes: a practical introduction to structure, mechanism and data analysis. 2nd ed. New York, NY: Wiley-VCH Inc; 2000:305-317.
26. Collin N, Assumpcao TC, Mizurini DM, et al. Lufaxin, a novel factor Xa inhibitor from the salivary gland of the sand fly Lutzomyia longipalpis blocks protease-activated receptor 2 activation and inhibits inflammation and thrombosis in vivo. *Arterioscler Thromb Vasc Biol.* 2012;32(9):2185-2198.
27. Leavitt S, Freire E. Direct measurement of protein binding energetics by isothermal titration calorimetry. *Curr Opin Struct Biol.* 2001;11(5): 560-566.
28. Emsley J, McEwan PA, Gailani D. Structure and function of factor XI. *Blood.* 2010;115(13): 2569-2577.
29. Hackeng TM, Sere KM, Tans G, Rosing J. Protein S stimulates inhibition of the tissue factor pathway by tissue factor pathway inhibitor. *Proc Natl Acad Sci USA.* 2006;103(9):3106-3111.
30. Ndonwi M, Tuley EA, Broze GJ Jr. The Kunitz-3 domain of TFPI-alpha is required for protein S-dependent enhancement of factor Xa inhibition. *Blood.* 2010;116(8):1344-1351.

31. Muller F, Mutch NJ, Schenk WA, et al. Platelet polyphosphates are proinflammatory and procoagulant mediators in vivo. *Cell.* 2009;139(6): 1143-1156.
32. Cirino G, Cicala C, Bucci M, et al. Factor Xa as an interface between coagulation and inflammation. Molecular mimicry of factor Xa association with effector cell protease receptor-1 induces acute inflammation in vivo. *J Clin Invest.* 1997;99(10): 2446-2451.
33. Decrem Y, Rath G, Blasioli V, et al. Ir-CPI, a coagulation contact phase inhibitor from the tick Ixodes ricinus, inhibits thrombus formation without impairing hemostasis. *J Exp Med.* 2009;206(11): 2381-2395.
34. Wesselschmidt R, Likert K, Huang Z, MacPhail L, Broze GJ Jr. Structural requirements for tissue factor pathway inhibitor interactions with factor Xa and heparin. *Blood Coagul Fibrinolysis.* 1993; 4(5):661-669.
35. Wesselschmidt R, Likert K, Girard T, Wun TC, Broze GJ Jr. Tissue factor pathway inhibitor: the carboxy-terminus is required for optimal inhibition of factor Xa. *Blood.* 1992;79(8):2004-2010.
36. Yang L, Sun MF, Gailani D, Rezaie AR. Characterization of a heparin-binding site on the catalytic domain of factor XIa: mechanism of heparin acceleration of factor XIa inhibition by the serpins antithrombin and C1-inhibitor. *Biochemistry.* 2009;48(7):1517-1524.
37. Mast AE, Broze GJ Jr. Physiological concentrations of tissue factor pathway inhibitor do not inhibit prothrombinase. *Blood.* 1996;87(5): 1845-1850.
38. Smith RP, Higuchi DA, Broze GJ Jr. Platelet coagulation factor XIa-inhibitor, a form of Alzheimer amyloid precursor protein. *Science.* 1990;248(4959):1126-1128.
39. Navaneetham D, Jin L, Pandey P, et al. Structural and mutational analyses of the molecular interactions between the catalytic domain of factor XIa and the Kunitz protease inhibitor domain of protease nexin 2. *J Biol Chem.* 2005;280(43): 36165-36175.
40. Oschatz C, Maas C, Lecher B, et al. Mast cells increase vascular permeability by heparin-initiated bradykinin formation in vivo. *Immunity.* 2011; 34(2):258-268.
41. Nieswandt B, Kleinschnitz C, Stoll G. Ischaemic stroke: a thrombo-inflammatory disease? *J Physiol.* 2011;589(Pt 17):4115-4123.
42. Massberg S, Grahl L, von Bruehl ML, et al. Reciprocal coupling of coagulation and innate immunity via neutrophil serine proteases. *Nat Med.* 2010;16(8):887-896.
43. Rosen ED, Gailani D, Castellino FJ. FXI is essential for thrombus formation following FeCl3-induced injury of the carotid artery in the mouse. *Thromb Haemost.* 2002;87(4):774-776.
44. Ledizet M, Harrison LM, Koskia RA, Cappello M. Discovery and pre-clinical development of antithrombotics from hematophagous invertebrates. *Curr Med Chem Cardiovasc Hematol Agents.* 2005;3(1):1-10.
45. Mizurini DM, Francischetti IM, Andersen JF, Monteiro RQ. Nitrophorin 2, a factor IX(a)-directed anticoagulant, inhibits arterial thrombosis without impairing haemostasis. *Thromb Haemost.* 2010; 104(6):1116-1123.
46. Gailani D, Lasky NM, Broze GJ Jr. A murine model of factor XI deficiency. *Blood Coagul Fibrinolysis.* 1997;8(2):134-144.
47. Schumacher WA, Luettgen JM, Quan ML, Seiffert DA. Inhibition of factor XIa as a new approach to anticoagulation. *Arterioscler Thromb Vasc Biol.* 2010;30(3):388-392.
48. Zhang H, Lowenberg EC, Crosby JR, et al. Inhibition of the intrinsic coagulation pathway factor XI by antisense oligonucleotides: a novel antithrombotic strategy with lowered bleeding risk. *Blood.* 2010;116(22): 4684-4692.
49. Wu W, Li H, Navaneetham D, Reichenbach ZW, Tuma RF, Walsh PN. The kunitz protease inhibitor domain of protease nexin-2 inhibits factor XIa and murine carotid artery and middle cerebral artery thrombosis. *Blood.* 2012;120(3):671-677.
50. Hagedorn I, Schmidbauer S, Pleines I, et al. Factor XIIa inhibitor recombinant human albumin Infestin-4 abolishes occlusive arterial thrombus formation without affecting bleeding. *Circulation.* 2010;121(13):1510-1517.